



# The Calibration Home Base for Imaging Spectrometers

Deutsches Zentrum für Luft- und Raumfahrt e.V.,  
Remote Sensing Technology Institute\*

## Instrument Scientists:

- Johannes Brachmann, IMF, DLR Oberpfaffenhofen  
phone: +49 8153 281427, email: [Johannes.Brachmann@dlr.de](mailto:Johannes.Brachmann@dlr.de)
- Andreas Baumgartner, IMF, DLR Oberpfaffenhofen  
phone: +49 8153 281402, email: [Andreas.Baumgartner@dlr.de](mailto:Andreas.Baumgartner@dlr.de)
- Peter Gege, IMF, DLR Oberpfaffenhofen  
phone: +49 8153 281242, email: [Peter.Gege@dlr.de](mailto:Peter.Gege@dlr.de)

**Abstract:** The Calibration Home Base (CHB) is an optical laboratory designed for the calibration of imaging spectrometers for the VNIR/SWIR wavelength range. Radiometric, spectral and geometric calibration as well as the characterization of sensor signal dependency on polarization are realized in a precise and highly automated fashion. This allows to carry out a wide range of time consuming measurements in an efficient way. The implementation of ISO 9001 standards in all procedures ensures a traceable quality of results. Spectral measurements in the wavelength range 380–1000 nm are performed to a wavelength uncertainty of  $\pm 0.1$  nm, while an uncertainty of  $\pm 0.2$  nm is reached in the wavelength range 1000–2500 nm. Geometric measurements are performed at increments of  $1.7 \mu\text{rad}$  across track and  $7.6 \mu\text{rad}$  along track. Radiometric measurements reach an absolute uncertainty of  $\pm 3\%$  ( $k=1$ ). Sensor artifacts, such as caused by stray light will be characterizable and correctable in the near future. For now, the CHB is suitable for the characterization of pushbroom sensors, spectrometers and cameras. However, it is planned to extend the CHBs capabilities in the near future such that snapshot hyperspectral imagers can be characterized as well. The calibration services of the CHB are open to third party customers from research institutes as well as industry.

\*Cite article as: DLR Remote Sensing Technology Institute. (2016). The Calibration Home Base for Imaging Spectrometers. *Journal of large-scale research facilities*, 2, A82. <http://dx.doi.org/10.17815/jlsrf-2-137>



## 1 Introduction

The Calibration Home Base (CHB) is an optical laboratory developed and operated by the German Aerospace Center (DLR) Oberpfaffenhofen for the calibration of (airborne) hyperspectral sensors and field spectrometers. Radiometric and spectral characterization of cameras is carried out as well. The CHB is made available to public through the user service Optical Airborne Remote Sensing and Calibration Home Base (OpAiRS) (for contact details see Sec. 6).

The CHB was partly funded by the European Space Agency (ESA) to establish a calibration facility for the airborne imaging spectrometer APEX (Itten et al., 2008; Schaepman et al., 2015), but is used for other optical sensors as well. NEO HySpex VNIR-1600 and SWIR-320me sensors, which are owned by DLRs Remote Sensing Technology Institute (DLR-IMF) are regularly calibrated in the facility (Lenhard, Baumgartner, & Schwarzmaier, 2015). It is the only facility in Europe which allows a precise characterization of the radiometric, geometric and spectral properties of bulky and heavy instruments up to 500 kg (including mechanical interface) in the wide spectral range 380–2500 nm. All standard measurements in the CHB are routinely carried out and are completely automatized. However, the CHB is also open to requests for special measurement campaigns, if communicated.

Pushbroom spectrometers have long been a standard design for airborne and satellite imaging spectrometers. These are in the main focus of the calibration activities in the CHB. They are, in effect, line scanners that need to be moved such that successively recorded data can be assembled to flight lines. Thus, two orthogonal directions are distinguished: Across-track data are recorded simultaneously in a direction orthogonal to the movement of the instrument. The total viewing angle in this direction is called field of view (FOV). Along-track data is successively recorded line-by-line in direction of the sensor movement. The viewing angle of each detector element is called instantaneous field of view (IFOV). The IFOV is similar to the along-track viewing angle.

In this paper, a short description of the CHB and its capabilities is given. A more complete description with technical details of the status of the facility as it was in 2009 can be found in Gege et al. (2009). Upgrades to the facility that have been made since are pointed out throughout the text.

The paper is structured as follows: In Sec. 2 standard measurements are described. A description of the laboratory and measurement setups is given in Sec. 3. To be characterizable by standard procedures in the CHB sensors must comply with the specifications summarized in Sec. 1. It is to be noted that the required specifications cover a very wide parameter range. Thus, almost all current imaging spectrometers will meet these requirements. In Sec. 6 a list of publications with context to recent activities in the CHB is mentioned.

## 2 Standard CHB Measurements

### 2.1 Spectral Measurements

Spectral measurements are performed with the monochromator setup described in Sec. 3.3.

The following sensor parameters are derived:

- Spectral Response Function  $SRF_{k,x}(\lambda)$  of selected pixels ( $x$ ) and selected channels ( $k$ ). Gives a normalized signal vs. wavelength  $\lambda$ .
- Center wavelength  $\lambda_{k,x}$  of selected channels and selected pixels. Gives the median of  $SRF_{k,x}(\lambda)$ .
- Spectral smile of a selected channel. Gives the center wavelength  $\lambda_{k,x}$  vs. the pixel number  $x$ .
- Spectral sampling distance of selected channels and selected pixels. Gives the wavelength difference  $|\lambda_{k+1,x} - \lambda_{k,x}|$  of adjacent channels.
- Spectral range of selected pixels. Gives the wavelength difference  $|\lambda_{N,x} - \lambda_{1,x}|$  of first and last channels.
- Full Width at Half Maximum (FWHM) of selected channels and selected pixels. Gives the wavelength interval corresponding to  $1/2 SRF_{k,x}(\lambda)$ . The FWHM is identical to the spectral resolution.

## 2.2 Geometric Measurements

Geometric measurements on imaging spectrometers as well as cameras are performed with the collimator setup described in Sec. 3.4. See Fig. 2 for the choice of a coordinate system. Images of targets (slits of various sizes) are moved in small steps across the detector elements.

If the sensor under investigation is a camera, the image of a target is geometrically similar to the target itself. However, for a pushbroom spectrometer across track (spatial direction) are different from along track (spectral direction of each frame) measurements.

The following sensor parameters can be derived:

- Line Spread Function across track ( $LSF_Y(\alpha)$ ) and along track ( $LSF_X(\beta)$ ): normalized signal of a detector element vs. across track angle  $\alpha$  and along track angle  $\beta$ , respectively.
- Center coordinates (across track angle  $\alpha_x$ , along track angle  $\beta_x$ ) of selected pixels (pixel number  $x$ ): angles corresponding to the signal at the median of  $LSF_Y(\alpha)$  and  $LSF_X(\beta)$ .
- Across track sampling distance: angle difference  $|\alpha_{x+1} - \alpha_x|$  of adjacent pixels.
- IFOV of selected pixels across track. This corresponds to an angle interval of  $1/2 LSF_Y(\alpha)$  and  $1/2 LSF_X(\beta)$ , respectively. The IFOV is defined as the FWHM.
- FOV across track and along track.  $FOV_Y$  is the across track angle difference  $|\alpha_1 - \alpha_N|$  of first and last pixel,  $FOV_X$  is identical to  $IFOV_X$ .
- Modulation transfer functions are calculated from measured line spread functions.

## 2.3 Radiometric Measurements

The task of radiometric calibration is the conversion of sensor signals from sensor units C (digital numbers, DN) to physical units L (spectral radiance,  $W/(m^2 nm sr)$ ). For these measurements, our radiometric standard (Schwarzmaier et al., 2012) and two integrating spheres are available. The setup for radiometric measurements is described in Sec. 3.5.

The following measurements that are connected to a sensor's radiometric response are carried out in the CHB:

- Absolute radiometric response at one fixed illumination  $r_{k,x}(\lambda)$  of selected pixels (number  $x$ ) and all channels (number  $k$ ) in the spectral range 380 – 2500 nm.
- Relative radiometric response at one fixed illumination  $r_{k,x'}/r_{k,x}$  of all pixels and all channels in the spectral range 380 – 2500 nm.

## 2.4 Polarization Dependency

Polarization sensitivity of sensors in the wavelength range 380 – 2500 nm is investigated with the setup shortly described in Sec. 3.6.

## 3 Laboratory Infrastructure

The optical laboratory has a size of  $12.8 \times 5.5$  m with a height of 8 m and can be darkened. The entrance door (2.3 m width, 4.10 m height) and a crane, which is mounted on the ceiling, allow for an easy handling of larger equipment. Air-conditioning keeps the temperature at  $20 \pm 1^\circ C$  and meta-data such as temperature, pressure, and humidity is recorded.

Fig. 1 shows a picture of the facility and the main measurement equipment. Detailed descriptions of the components are given in the following.

### 3.1 Calibration Bench

The calibration bench (see Fig. 1) is made of granite. It provides a working area of  $3 \times 1.6$  m. The surface was polished to a maximum deviation from flatness of  $1.24 \mu m$  at the area where the folding mirror (see Sec. 3.2) is attached.



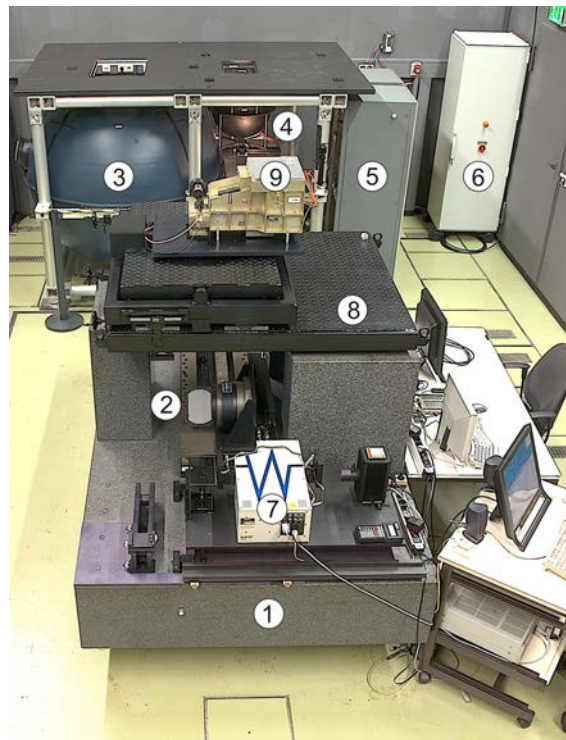


Figure 1: Calibration Home Base (CHB). ① Calibration bench, ② Folding mirror, ③ Large integrating sphere, ④ Small integrating sphere, ⑤ Power supplies of large integrating sphere, ⑥ Control electronics of folding mirror, ⑦ Monochromator, ⑧ CHB adapter, ⑨ Exemplary sensor.

Technical details and make of the calibration bench are given in Gege et al. (2009). For vibrational decoupling from the building the calibration bench rests on a concrete block of approximately 50 tons. This block is very well vibrationally isolated from the building.

As a core hardware component the calibration bench is hosting the components for geometric, spectral and stray light measurements. It is especially adapted to heavyweight instruments up to 350 kg. The concept of Gege et al. (2009); Sümnich (2003) is illustrated in Fig. 2. The sensor is mounted in a fixed position on top of 3 pillars ②, downward looking to a mirror ④, which reflects either the beam for geometric ⑤ or for spectral ⑥ measurements into the instrument. This ‘folding mirror’ can be tilted in across-track direction of the sensor in order to set the angle of incidence, and it can be moved in the horizontal direction to meet the entrance aperture. The sensor is attached and aligned on the calibration bench using an adapter. Adapters can be supplied by customers or the general purpose adapter shown in Fig. 3 will be made available. The latter is designed to carry loads of up to 150 kg and is described in detail in Gege et al. (2009).

### 3.2 Folding Mirror

A central component on the calibration bench is a mirror which performs coupled linear and rotary movements, called the folding mirror (see Figs. 1, 2). A summary of the technical specifications is given in Gege et al. (2009).

The mirror has a usable area of rectangular shape with axis lengths of  $174 \times 114 \text{ mm}^2$ . It is made of Zerodur, the surface is silver to minimize changes of the polarization properties of the reflected radiation.

Mirror movements are realized very precisely by means of two air-bearing stages: a rotary stage is mounted on top of a linear stage. The linear stage defines the Y-axis of the calibration bench’s coordinate system (see Fig.2). The folding mirror assembly can be moved along the Y-axis by  $\pm 375 \text{ mm}$

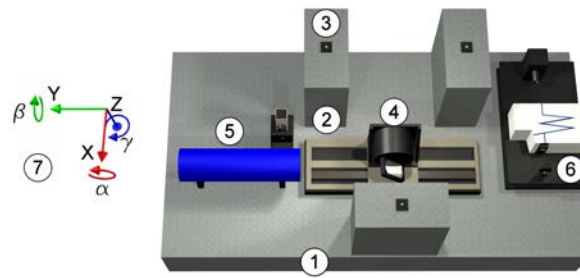


Figure 2: Setup for geometric and spectral measurements. ① Calibration bench, ② Pillar carrying sensor, ③ Interface plate, ④ Folding mirror, ⑤ Components for geometric measurements, ⑥ Components for spectral measurements, ⑦ Sensor coordinate system.



Figure 3: General purpose adapter available for sensor mounting. ① Opening for sensor baffle (covered); ② Flanges of different size to mount sensor; ③ Sliding rule to read the X setting; ④ Meters to read the settings of  $\beta$  and  $\gamma$ ;  $\textcircled{X}$ ,  $\textcircled{\beta}$ ,  $\textcircled{\gamma}$ : Hand wheels to align the indicated axes.

relative to the position where a nadir oriented sensor axis meets the linear stage. For the rotary stage angles are measured relative to the optical axis of a nadir oriented sensor. The rotary stage can be rotated by  $360^\circ$ . At  $90^\circ$  it is facing towards the monochromator, at  $270^\circ$  towards the collimator. Angular uncertainties are  $\pm 7 \mu\text{rad}$  for the pitch angle  $\alpha$ ,  $\pm 6 \mu\text{rad}$  for the roll angle  $\beta$ , and  $\pm 8 \mu\text{rad}$  for the yaw angle  $\gamma$ .

### 3.3 Monochromator Setup

For spectral measurements a monochromator generates a spectrally narrow-band beam of light which is reflected by the folding mirror at well-defined angles into the entrance aperture of the instrument. The setup is illustrated in Fig. 4. For the sake of simplicity the setup is illustrated with a linear arrangement of all components.

A QTH lamp (LOT-Oriel: 15 V, 150 W) powered by a stabilized DC power supply is used as a radiation source ①. After filtering out short wavelengths by use of a long pass filter (order filter) ② the radiation enters the monochromator, whose main components are the entrance slit ③, grating ⑤ and exit slit ⑦. The nearly monochromatic beam exiting the monochromator can be attenuated using a neutral density filter that is additionally mounted at ②. A recent update to the setup is the insertion of a short multimode optical fiber into the beam path at ⑨. This ensures that the beam entering the sensor after passing the folding mirror does not contain spectral – spatial correlations. The monochromator (Oriel MS257TM) is an asymmetrical Czerny-Turner design. It is equipped with a turret that can hold up to 4 gratings to cover different spectral ranges. The gratings are changed by turning the turret under software control.

Spectral measurements require that the beam coming from the monochromator overfills both the sensor's entrance aperture and its IFOV. In standard configuration the beam size at the detector entrance

aperture is approximately 7 cm, while an IFOV of up to 8.5 mrad is illuminated. However, if required, the mirror – optical fiber (⑨ – ⑩) combination can be adapted to a sensor and measurement task.

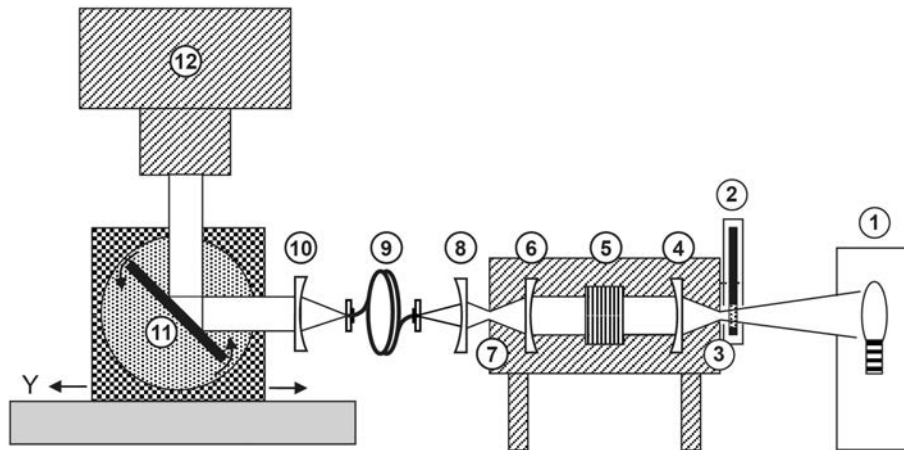


Figure 4: Monochromator setup for spectral measurements. ① Lamp, ② Long pass and/or neutral density filter in turnable wheel, ③ Entrance slit, ④, ⑥, ⑧, ⑩ Parabolic mirror, ⑤ Grating mounted on turret, ⑦ Exit slit, ⑨ Optical fiber, ⑪ Folding mirror, ⑫ Sensor.

### 3.4 Collimator Setup

The collimator setup is used for geometric calibration supplying a nearly parallel beam formed by a lamp-slit-collimator combination. A schematic sketch of the measurement setup is given in Fig.5. For the sake of simplicity the setup is illustrated with a linear arrangement of all components, while in reality the components ① and ② are mounted on the calibration bench at 90° relative to the others (see Fig. 2).

A lamp ① illuminates a turnable wheel ②. The wheel can be rotated in steps of 0.17 mrad using a rotary stage. Three slits of 50, 100 and 1000  $\mu\text{m}$  width and 10 mm length are mounted radially on the wheel, three similar slits with identical dimensions are aligned tangentially with respect to the axis of rotation. These slits are used as calibration targets. They can be moved in Y-direction by turning the folding mirror in small angle intervals and in the X-direction by moving the slit.

Slits are located at the focal plane of a collimator ④, whose parabolic mirror ③ forms a beam of almost parallel light. This beam is reflected from the folding mirror ⑤ into the entrance aperture of the sensor ⑥. The parabolic mirror has a focal length of 750 mm and produces a beam with divergence ( $\simeq s/f$ ), where  $s$  is the width of the slit.

**For across track measurements** a slit mounted tangentially on the wheel (corresponding to the sensor's X-direction) is used as the calibration target. Due to its height of 10 mm the beam has a divergence of 13 mrad in the along track direction, which overfills the IFOV of typical imaging spectrometers completely in the along track direction, but only partially in the across track direction due to the narrow slit width (0.07 mrad for the 50 mm slit). Imaging spectrometers disperse the radiation and project it in the wavelength direction on the detector array. Since the lamp emits a broad-band spectrum, an illuminated line is formed on the detector array by the different wavelengths. Measurements are performed by moving this line in sub-pixel steps in the across track direction over individual detector elements (pixels) using the folding mirror. In this way pixel response is determined as a function of the across track angle.

**For along track measurements** a slit mounted radially on the wheel is used as calibration target. Its height of 10 mm produces a beam of 13 mrad divergence in the across track direction which illuminates a number of adjacent pixels. Consequently, a broad band of spectrally dispersed light is projected on the focal plane. Due to the narrow slit width each illuminated pixel receives light in the along track

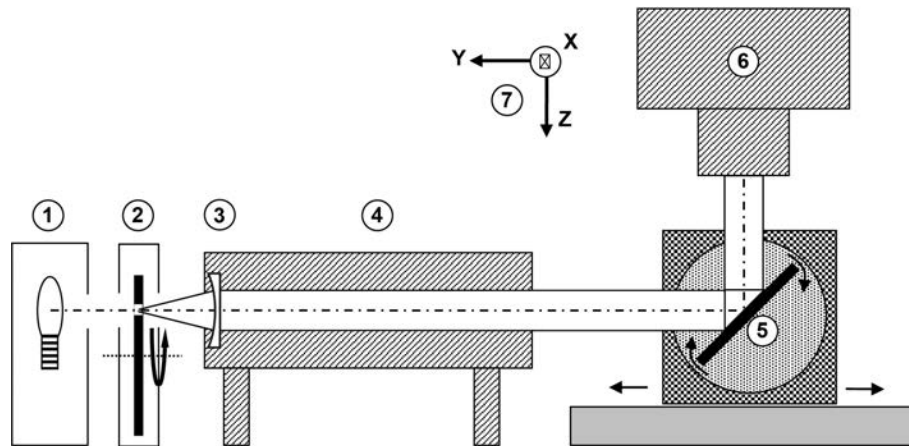


Figure 5: Setup for geometric measurements. ① Lamp, ② Slit in turnable wheel, ③ Parabolic mirror, ④ Collimator, ⑤ Folding mirror, ⑥ Sensor, ⑦ Sensor coordinate system.

direction only from a narrow angle interval. Measurements are performed by moving the beam in sub-pixel steps in the along track direction across the entrance slit by turning the slit wheel. In this way the pixel response is determined as a function of the along track angle. The minimum increment is  $\simeq \delta r/f = 7.6\mu\text{rad}$ . Here  $\delta = 170\mu\text{rad}$  is the minimum increment of the wheel,  $r = 32.5\text{ mm}$  is the wheel radius at the slit position and  $f = 750\text{ mm}$  is the focal length of the collimator.

### 3.5 Radiance Standards

Two integrating spheres are available for radiometric measurements (see Fig. 1). The sensor is mounted during the measurements on top of the frame either above the small sphere or above the large sphere, depending on the measurement task. The radiance spectrum of both spheres is traceable against German national standard. In order to achieve traceability, the radiance spectrum is constantly monitored against our radiometric standard (RASTA, calibrated at Physikalisch Technische Bundesanstalt) (Schwarzmaier et al., 2012) by the use of a transfer spectrometer (SVC HR1024i). The resulting radiometric spectral ( $k=1$ ) uncertainty is 2% in the spectral range 400–2500 nm.

**The large sphere** is used for sensors with large apertures. It has a diameter of 1.65 m and an aperture of  $55 \times 40\text{ cm}^2$  which can be reduced to  $20 \times 30\text{ cm}^2$  for higher radiance. It is equipped with 18 QTH lamps of different power, which are operated independently using 18 stabilized DC power supplies. The radiant exitance can be changed in various steps from 57 to  $1524\text{ W/m}^2$  by using different lamp combinations. The sphere offers a stability of better than 0.5% during a typical measurement period of 20 minutes.

**The small sphere's** angular integrated exitance is  $2309\text{ W/m}^2$ . The expanded uncertainty  $U(k=2)$  is 1% from 390 to 1700 nm. It increases towards shorter and longer wavelengths (Gege et al., 2009). The sphere has a diameter of 50 cm and an aperture of  $4 \times 20\text{ cm}$ . At the standard distance (sensor aperture at plane of CHB adapter flange) the sphere illuminates a FOV of  $\pm 12.5^\circ$ . Four 100 W QTH lamps are operated using a stabilized DC power supply.

### 3.6 Polarizer Setup

To analyze polarization sensitivity of the sensor under test, a wire grid polarizer (Moxtek UBB01A, open aperture  $\varnothing = 9\text{ cm}$ ) is mounted after the exit port of the large integrating sphere. Using the latter, all pixels and channels can be characterized simultaneously. A motorized rotation stage (Newport URS150BPP) is used to set angles of the linearly polarized radiation.

## 4 Requirements for Pushbroom Sensors

Tab. 1 summarizes specifications that are required for pushbroom sensors to be characterizable by standard CHB measurement procedures. However, the CHB is open to special requests for which some of the specifications given may be changed, if needed.

Sensor parameter	Range	Set-up, measurement task	Comment
Mass	<500 kg	Sensor + adapter	Using sensor specific adapter
	<150 kg	Sensor	Using CHB adapter
Spectral range	380–2500 nm	All standard measurements	Accessible spectral range
Spectral bandwidth	>1 nm	Spectral char. 380–1400 nm	Measurement condition: monochromator bandwidth <1/8 sensor bandwidth.
	>2 nm	Spectral char. 1400–2500 nm	
Aperture	$\varnothing < 5$ cm	Spectral char.	Depends on illumination of sensor aperture
	$\varnothing < 12$ cm	Geometric char.	
	$< 40 \times 55$ cm <sup>2</sup>	Radiometric char.	
IFOV	$\varnothing < 9$ cm	Polarization char.	Depends on illumination of sensor aperture
	<2 mrad	Spectral char.	
	>0.5 mrad	Geometric char.	
	>0.06 mrad	Geometric char.	
FOV	< 45°	Radiometric char.	Using large sphere & CHB adapter for sphere
	< 51°	Spectral char.	
	< 51°	Geometric char.	
	< 60°	Radiometric char.	Using large sphere & CHB adapter for sphere

Table 1: Required specifications for pushbroom sensors.

## 5 Conclusion and Outlook

The calibration laboratory for (airborne) imaging and field spectrometers at the German Aerospace Center in Oberpfaffenhofen has now been operational for 10 years. Within this time, the facility has witnessed constant update and improvement. The CHB offers a wide range of precision characterization measurements for spectrometers and cameras. The scope of these standard, fully automatized measurements is constantly extended to meet the needs of new types of sensors and in order to metrologically access more device parameters.

DLR-IMF will take part in the EnMAP satellite calibration and characterization campaign. Within this campaign, support for spectral, radiometric and geometric characterization measurements will be given. These are similar to standard measurements that are routinely carried out in the CHB. Further, the development of a concept, characterization and correction procedure for imaging imperfections, such as due to stray light, in the wavelength range 400–2500 nm is in the responsibility of DLR-IMF. The developed methods will also be available in the CHB.



Hyperspectral snapshot or single frame sensors offer the possibility to simultaneously acquire hyperspectral data in two dimensions. Recently, these rather new spectrometers have arisen much interest in the remote sensing community. Different designs are currently used for "smaller scale" observation such as by use of small unmanned aerial vehicles. In this context the CHBs measurement capabilities will be extended such that a standard measurement procedure for these new sensors will be implemented.

## 6 Selected Further Reading & Contact Details

- An overview of recent activities and advances in the CHB can be found in Lenhard (2015).
- On the improvement that can be achieved through thorough hyperspectral sensor calibration (Lenhard, Baumgartner, Gege, et al., 2015).
- On the traceability of the CHB radiometric standard (Taubert et al., 2013).
- On the calibration of the CHB monochromator (Schwarzmaier et al., 2013).
- For contact & information visit the OpAiRS website at <http://www.dlr.de/opairs>

## References

- Gege, P., Fries, J., Haschberger, P., Schötz, P., Schwarzer, H., Strobl, P., ... Vreeling, W. J. (2009). Calibration facility for airborne imaging spectrometers. *{ISPRS} Journal of Photogrammetry and Remote Sensing*, 64(4), 387 - 397. <http://dx.doi.org/10.1016/j.isprsjprs.2009.01.006>
- Itten, K. I., Dell'Endice, F., Hueni, A., Kneubühler, M., Schläpfer, D., Odermatt, D., ... Meuleman, K. (2008, Oktober). APEX - the hyperspectral ESA Airborne Prism Experiment. *Sensors*, 8(10), 6235 - 6259. <http://dx.doi.org/10.3390/s8106235>
- Lenhard, K. (2015). *Improving the calibration of airborne hyperspectral sensors for earth observation* (Thesis(Dissertation), University of Zurich, Germany). <http://elib.dlr.de/96632>.
- Lenhard, K., Baumgartner, A., Gege, P., Nevas, S., Nowy, S., & Sperling, A. (2015). Impact of improved calibration of a neo hypspx vnir-1600 sensor on remote sensing of water depth. *IEEE Transactions on Geoscience and Remote Sensing*, 53(11), 6085-6098. <http://dx.doi.org/10.1109/TGRS.2015.2431743>
- Lenhard, K., Baumgartner, A., & Schwarzmaier, T. (2015). Independent laboratory characterization of NEO HySpex Imaging Spectrometers VNIR-1600 and SWIR-320m-e. *IEEE Transactions on Geoscience and Remote Sensing*, 53(4), 1828-1841. <http://dx.doi.org/10.1109/TGRS.2014.2349737>
- Schaepman, M. E., Jehle, M., Hueni, A., D'Odorico, P., Damm, A., Weyermann, J., ... Itten, K. I. (2015). Advanced radiometry measurements and earth science applications with the airborne prism experiment (APEX). *Remote Sensing of Environment*, 158, 207 - 219. <http://dx.doi.org/10.1016/j.rse.2014.11.014>
- Schwarzmaier, T., Baumgartner, A., Gege, P., Kühler, C., & Lenhard, K. (2012). The Radiance Standard RASTA of DLR's calibration facility for airborne imaging spectrometers. *Proc. SPIE*, 8533, 85331U-85331U-6. <http://dx.doi.org/10.1117/12.974599>
- Schwarzmaier, T., Baumgartner, A., Gege, P., & Lenhard, K. (2013). Calibration of a monochromator using a lambdameter. *Proc. SPIE*, 8889, 888910-888910-6. <http://dx.doi.org/10.1117/12.2028670>
- Sümnich, K.-H. (2003). Vorrichtung zur Kalibrierung eines optischen Instruments mit einem fotoelektrischen Detektor. *German Patent Application Publication*. (Patentschrift DE 102 18 947 A 1)
- Taubert, D. R., Hollandt, J., Sperfeld, P., Pape, S., Höpe, A., Hauer, K.-O., ... Baumgartner, A. (2013). Providing radiometric traceability for the calibration home base of DLR by PTB. *AIP Conference Proceedings*, 1531(1), 376-379. <http://dx.doi.org/10.1063/1.4804785>

